

# Hydrotalcites: relation between structural features, basicity and activity in the Wittig reaction

M. Sychev<sup>a,\*</sup>, R. Prihod'ko<sup>a</sup>, K. Erdmann<sup>b</sup>, A. Mangel<sup>c</sup>, R.A. van Santen<sup>d</sup>

<sup>a</sup> Faculty of Chemical Technology, National Technical University of Ukraine, 03056, Kiev, pr. Peremogy 37, Ukraine

<sup>b</sup> Faculty of Chemistry, Nicholas Copernicus University, ul. Gagarina 7, 87-100 Torun, Poland

<sup>c</sup> C.I. Electronics Ltd., Brunel Road, Churchfields, Salisbury, Wiltshire SP2 7PX, UK

<sup>d</sup> Schuit Institute of Catalysis, Eindhoven University of Technology, Eindhoven, PO Box 513, 5600 MB Eindhoven, Netherlands

## Abstract

Carbonate hydrotalcites (HTIs) were prepared by coprecipitation of metal nitrate salts and  $\text{Na}_2\text{CO}_3$ . The structural features of noncalcined, calcined and reconstructed materials were characterized by XRD,  $^{27}\text{Al}$  MAS NMR, AAS and  $\text{N}_2$  adsorption. It was shown that reconstruction of the calcined HTIs due to a memory effect results in the formation of materials with structural and surface features different from those of the parent hydrotalcites.

Hydrotalcites can efficiently catalyze the liquid-phase synthesis of alkenes following the Wittig reaction. The optimum activity was found for materials with the  $\text{Al}/(\text{Al} + \text{M}^{2+})$  molar ratio of 0.20–0.26. Their selectivity can be controlled by a proper choice of pretreatment conditions, such as calcination and structural reconstruction. The solvent composition influences both the reaction rate and catalyst selectivity. The *Z*- and *E*-alkenes can be obtained with a high yield. The applicability of HTIs for the Wittig reaction is limited by the  $pK_a$  and composition of the ylide precursor. The Wittig reaction is sensitive to the structure of the basic catalyst when a moderate acid, such as  $\text{Ph}_3\text{P}^+\text{CH}_2\text{CO}_2\text{Et}$  with  $pK_a = 8.8$ , is used as the ylide precursor. © 2001 Elsevier Science B.V. All rights reserved.

**Keywords:** hydrotalcites; structural reconstruction; basicity; alcohol decomposition; Wittig reaction

## 1. Introduction

Basicity of hydrotalcite-like compounds (HTIs) depends mainly on both the nature of the structure-constituting cations and the kind of interlayer anions (Cavani et al., 1991; Rao et al., 1998) stimulates their use in base-catalyzed reactions to produce less polluting processes. In most catalytic applications, HTIs are used in the calcined form consisting of

highly homogeneous nonstoichiometric mixture of metal oxides (Cavani et al., 1991). Studies on the catalysis over as-synthesized hydrotalcites have been reported as well (e.g. Choudary et al., 1997; Watanabe and Tatsumi, 1998). Some examples of the use of hydrotalcites as active and selective catalysts in various base-catalyzed liquid-phase reactions have been reported in recent years (Climent et al., 1995, 1999; Kumbhar et al., 1998; Kaneda et al., 1995; Rao et al., 1998).

The Wittig reaction is one of the most important processes in the organic chemistry for synthesizing alkenes with unambiguous positioning of the double

\* Corresponding author. Tel.: +380-44-441-1279; fax: +380-44-274-2004.

E-mail address: sytsh@xtf.ntu-kpi.kiev.ua (M. Sychev).

bond (Hwang et al., 1999). The reaction involves interaction of phosphonium ylide with an aldehyde or a ketone (Shen, 1998). The reacting ylide is formed from a phosphonium salt in a solution of a base, such as *n*-BuLi, NaH, *t*-BuOK, and NaOH (Climent et al., 1989; Hwang et al., 1999), or under phase-transfer conditions when a solid base, e.g. Ba(OH)<sub>2</sub>, MgO or ZnO, is used (Climent et al., 1989).

The above findings encouraged us to use HTIs as basic catalysts for the Wittig reaction. We have studied the influence of structural transformations of Mg- and Zn-containing HTIs on their behavior in the Wittig reaction with the aim of establishing the correlation between their activity and selectivity, and the composition, textural features and basicity of those materials. The catalysts were thoroughly characterized as well.

## 2. Experimental

### 2.1. Preparation

The Mg–Al HTIs with the Mg/Al molar ratios of 2, 3, and 5 were prepared as described by Velu and Swamy (1994) using the metal nitrates. The obtained materials are designated as Mg<sub>2</sub>Al, Mg<sub>3</sub>Al, and Mg<sub>5</sub>Al, respectively. Zn–Al HTIs were prepared under conditions of low supersaturation (Cavani et al., 1991). These materials are referred to as Zn<sub>2</sub>Al, Zn<sub>3</sub>Al, and Zn<sub>5</sub>Al, where the numbers indicate the Zn/Al molar ratios.

The Mg, Zn, and Al contents in the prepared HTIs were determined by the atomic absorption spectroscopy (AAS). Calcination of the samples was carried out under shallow-bed conditions in an air-flow, with the oven temperature increasing up to 723, 773, 823 or 923 K at a rate of 3 K/min. The final temperature was maintained for 5 h. After cooling down to ambient temperature, the materials were stored in closed containers under Ar, and are denoted with the index (C).

Reconstruction of the hydrotalcite-like structure was performed as described by Watanabe and Tsumi (1998). One gram of a calcined material was stirred in 100 ml of distilled water at 373 K for 40 min, and then dried at 383 K overnight. These samples are denoted with the index (R). The chemi-

cal formulae and structural parameters of the parent, reconstructed and calcined materials (BET surface area) are given in Table 1.

### 2.2. Characterization techniques

X-ray diffraction (XRD) patterns of oriented powdered samples were recorded on a DRON-3 diffractometer using CuK<sub>α</sub> radiation ( $\lambda = 0.154178$  nm). The crystallite size ( $\epsilon$ ) was derived from the Sherrer equation. A true half-width of the X-ray reflection ( $b$ ) was calculated from the relation:  $b = (B - b^2)/B$ , with  $B$  being the half-maximum peak width, and  $b$  the instrument reflection width determined by using high-purity silica.

The <sup>27</sup>Al MAS NMR experiments were carried out on a Bruker AMX 300 WB spectrometer with the high-power proton decoupling, using a standard 7-mm o.d. ZrO<sub>2</sub> rotor. The spectra were recorded at 78.20 MHz, and the recycle time was 2 s. An aqueous solution of Al(NO<sub>3</sub>)<sub>3</sub> was used as a reference. To avoid the rehydration, freshly calcined samples were stored under dry argon in the glass-soldered ampoule and then used for NMR experiments.

The BET specific surface areas were calculated from the N<sub>2</sub> adsorption isotherms taken at 77 K (sample outgassed at 473 K, 10<sup>-4</sup> mbar, 5 h) using a Micromeritics ASAP 2010 facility.

### 2.3. Catalysis

Conditions of the Wittig reaction: aldehyde (0.97 mmol), a phosphonium salt (0.97 mmol) synthesized according to Hwang et al. (1999), 20 mg of a catalyst and 2 ml of solvent were mixed and heated under stirring at 333 K during the reaction. The reaction mixture was then separated from the catalyst by centrifugation, and the products deposited on the catalyst were removed by washing with ethanol. The composition of the resulting liquid was analyzed by GLC, GC-MS (GC-17A, Shimadzu), and <sup>1</sup>H NMR.

## 3. Results and discussion

### 3.1. Characterization of hydrotalcite transformations

The XRD patterns of the noncalcined HTIs showed the characteristic lamellar structure. A satisfactory

Table 1  
Chemical formulae,  $M^{2+}/Al^{3+}$  molar ratios, structural parameter ( $a$ ), crystallite size ( $\varepsilon$ ) of parent and reconstructed HTIs, and BET surface area,  $S_{BET}(C)$ , of materials calcined at 773 K

Sample	Formula	$M^{2+}/Al^{3+}$	$x$ (Al/Al + $M^{2+}$ )	$a$ , nm	$\varepsilon$ , nm	$d$ , nm	$\varepsilon'$ , nm	$S_{BET}(C)$ ( $m^2 g^{-1}$ )
Mg2Al	$[Mg_{0.668}Al_{0.332}(OH)_2](CO_3)_{0.166} \cdot 0.56 H_2O$	2.01	0.332	0.3042	18.5	0.3046	34.6	172
Mg3Al	$[Mg_{0.751}Al_{0.249}(OH)_2](CO_3)_{0.125} \cdot 0.62 H_2O$	3.02	0.249	0.3061	19.9	0.3063	22.7	164
Mg5Al	$[Mg_{0.833}Al_{0.167}(OH)_2](CO_3)_{0.084} \cdot 0.64 H_2O$	4.98	0.167	0.3086	20.7	0.3088	18.4	155
Zn2Al	$[Zn_{0.669}Al_{0.331}(OH)_2](CO_3)_{0.166} \cdot 0.46 H_2O$	2.02	0.331	0.3071	44.8	0.3069	21.6	78
Zn3Al	$[Zn_{0.748}Al_{0.252}(OH)_2](CO_3)_{0.126} \cdot 0.45 H_2O$	2.97	0.252	0.3080	40.3	0.3072	28.9	73
Zn5Al	$[Zn_{0.837}Al_{0.136}(OH)_2](CO_3)_{0.081} \cdot 0.43 H_2O$	5.13	0.163	0.3088	47.0	0.3075	29.7	61

$d$  and  $\varepsilon'$  parameters of reconstructed samples.

correlation between lattice parameter  $a$  and values of  $x = Al/(Al + M^{2+})$  was found, confirming also the formation of the hydrotalcite-like structure. Increasing the  $M^{2+}$ -cation content results in an increase of the HTIs crystallite size ( $\varepsilon$ ) in the (110) direction (Table 1). Calcination of HTIs at temperatures above 723 K results in the formation of poorly crystallized Mg(Al)O and Zn(Al)O double oxides (Hudson et al., 1995).

Their hydration leads to the general regeneration of the original HT-like structure, as indicated by XRD. However, HTIs with a high  $M^{2+}$  concentration contain some residual oxide, as is detected by some peak broadening between  $2\theta = 30-60^\circ$  reflecting also a lower structural order than in the parent material. This tendency becomes more pronounced for the samples derived from precursors calcined at higher temperatures, especially for Zn–Al HTIs. For HTIs(R), the relation between  $a$  and  $x$  is nearly the same as that for the parent materials (Table 1). The reconstructed Mg–Al HTIs show that the  $\varepsilon$  vs.  $x$  relation is completely variant from those of noncalcined material (Table 1). The lower the Mg content, the larger the crystallites of Mg–Al HTIs(R). On the contrary, variation of the Zn concentration affects less the crystallite size of Zn–Al HTIs(R), which is lower than that of the parent materials (Table 1). Most likely, some  $Al^{3+}$  or  $Zn^{2+}$  cations cannot be transformed back to the original state inherent in the hydrotalcite structure.

Following on from the XRD results, MAS NMR was employed to study the influence of the calcination temperature and composition (for Mg–Al HTIs and Zn–Al HTIs, respectively) on their reconstruction behavior.

$^{27}Al$  MAS NMR spectra of noncalcined HTIs are similar to those reported in the literature (e.g. Beres et al., 1999). Calcination of Mg–Al HTIs results in the appearance of an additional peak at 74 ppm assigned to tetrahedrally coordinated aluminum, Al(tet). In addition to the appearance of the Al(tet) resonance, increasing the calcination temperature results in the change in the position of the Al(oct) peak maximum. The peak shifts from 7.9 ppm for the parent sample to ca. 15.0 ppm for the samples calcined at 723–923 K (Fig. 1A). This variation in the chemical shift indicates deformation of the coordination sphere of Al(oct) that influences also the

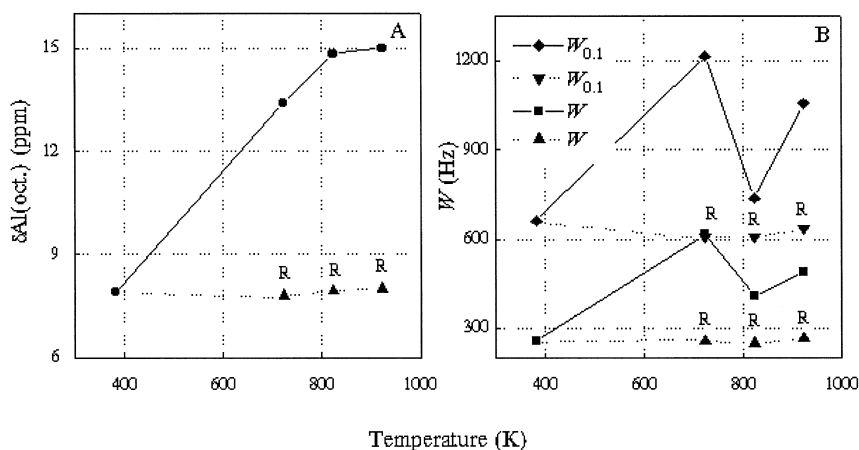


Fig. 1. Octahedral  $^{27}\text{Al}$  MAS NMR parameters for Mg<sub>3</sub>Al heated at various temperatures. (A) Position of peak maximum. (B) Peak width at half height,  $W$ , and at one-tenth height,  $W_{0.1}$ . R stands for the reconstructed samples.

neighboring octahedral Mg (Rey et al., 1992; Hudson et al., 1995; MacKenzie et al., 1993). In Fig. 1B, the peak width at half height ( $W$ ), and at one-tenth height ( $W_{0.1}$ ) that reflect the Al order (MacKenzie et al., 1993) are plotted vs. calcination temperature. These parameters increase with the heating temperature, showing a maximum at 723 K. Since the  $W_{0.1}$  parameter reflects the magnitude of the distribution of the electric field gradients (MacKenzie et al., 1993), these results are evidence of an increase in disorder for heating temperatures between 383 and 773 K.  $^{27}\text{Al}$  MAS NMR spectra of reconstructed Mg–Al HTIs contain a single resonance at 7.8–8.0 ppm (Fig. 1A). Its width ( $W$  and  $W_{0.1}$ ) does not significantly deviate from that of the noncalcined material (Fig. 1B). However, the  $^{27}\text{Al}$  NMR spectrum of Mg<sub>3</sub>Al(R) obtained from its precursor calcined at 923 K shows some broadening of the Al(oct) resonance. This reflects a partial disorder of such Al, caused obviously by some distortion in the reconstructed HTI structure.

Calcination of Zn–Al HTIs at 773 K causes significant changes in the coordination state of aluminum. The contribution of the Al(tet) resonance is noticeably larger compared to the Mg-containing HTIs. Soled et al. (1998) found that double oxides derived from Zn–Al HTIs contain Al primarily in tetrahedral sites whereas calcined Mg–Al materials contain Al primarily in octahedral positions. The

width ( $W$  and  $W_{0.1}$ ) of the Al(tet) resonance depends on the aluminum content, being the narrowest for the Zn<sub>5</sub>Al sample (Fig. 2). Moreover, two distinct lines (at ca. 14 and 0–5 ppm) of Al(oct) resonance could be detected in the NMR spectra of Zn–Al HTIs(C) (Fig. 2). According to Hudson et al. (1995), the two octahedral sites are principally Al(OH)<sub>6</sub>, probably with and without associated carbonate.

The observed change in the aluminum coordination could affect the neighboring octahedral Zn, analogously to the Mg-containing materials. Such a change, being more significant than for Mg–Al HTIs, might result in the formation of a larger amount of the segregated ZnO phase.

In the  $^{27}\text{Al}$  MAS NMR spectra of the reconstructed Zn–Al HTIs, only the Al(oct) resonance is observed, being narrower and more intense than that of the parent hydrotalcites. Apparently, in this case, the structure reconstruction leads to the diminution of distortions in the octahedral arrangements of the coordinating atoms and mean Al–O bond lengths. However, the existence of separate ZnO or Zn(OH)<sub>2</sub> cannot be excluded, even though discrete compounds are not distinguishable by XRD.

The above results demonstrate that reconstruction of calcined HTIs is a complex process resulting in the formation of materials with structural features and surface properties different from those of parent hydrotalcites.

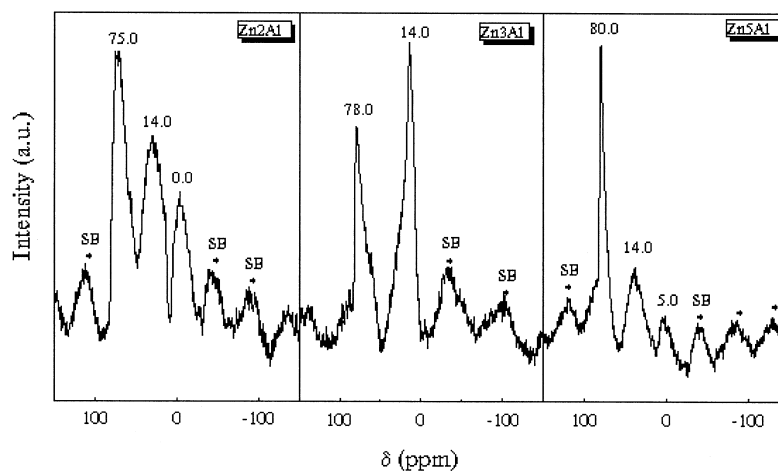


Fig. 2.  $^{27}\text{Al}$  MAS NMR spectra of Zn–Al HTIs calcined at 773 K.

### 3.2. The Wittig reaction

To perform the Wittig reaction (Fig. 3), 1,4-dioxane, ethanol (EtOH) and isobutanol (i-BuOH) were chosen as the solvents because of different polarity.

When EtOH or dioxane are used, the noncalcined HTIs show a low activity. Calcination of HTIs at 773 K results in a significant increase in the activity, which shows that the basicity is enough to produce phosphonium ylide. The decreased Al content leads to the increase in activity (Fig. 4). Recently, Climent et al. (1995) demonstrated that the proportion of the

stronger basic sites of HTIs(C) increases with increasing Al content in the brucite-like layers. At the same time, the total number of such sites tends to decrease. Most likely, in the case of hydrotalcite catalyzed Wittig reaction, the increasing number of basic sites results in a higher conversion of phosphonium salt.

The lower activity of Zn–Al HTIs(C) can be explained, at least in part, by the lower surface area and the larger crystallite size of these materials.

EtOH leads to a high percentage of the secondary process, the acetalization reaction with aldehyde,

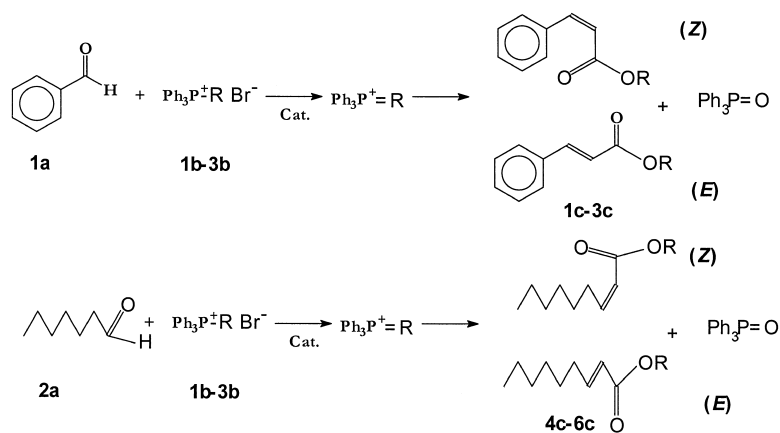


Fig. 3. Schematic representation of Wittig reaction.

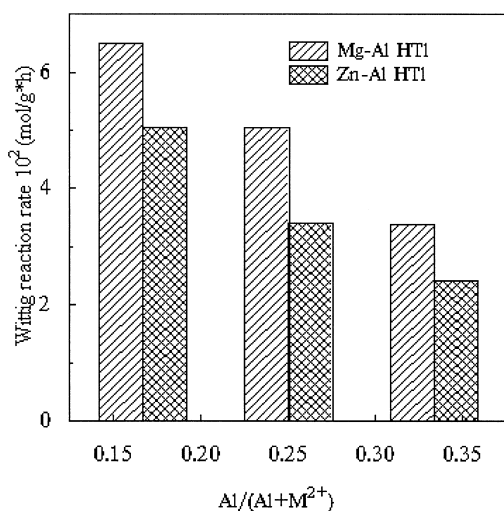


Fig. 4. Influence of the catalyst composition on the Wittig reaction rate. All catalyst were calcined at 773 K.

resulting in acetal formation over weak acid sites originating from alumina. Therefore, 1,4-dioxane is a solvent more suitable for the HTI catalyzed Wittig reaction. The presence of a small amount of water (5 vol.%) in dioxane increases the reaction rate, while excess water reduces the reaction rate. According to Climent et al. (1989), water plays an important role in the decomposition of the oxaphosphetane intermediate.

The HTIs(R) samples behave quite differently from the calcined materials. Mg–Al HTIs(R) are almost inactive, whereas those containing Zn, e.g. Zn5Al(R), exhibit a moderate or high activity. We can speculate that this is caused by the microcrystalline phase of ZnO resulting from an incomplete structural reconstruction. This phase is known to be highly active (Moison et al., 1987). ZnO (a reference sample) was completely dissolved when **1b** was used as the ylide precursor. Therefore, we assume that the rate-controlling step is the ylide formation on the solid surface.

Over the Zn5Al(R) catalyst, the reaction seems to proceed in the homogeneous phase near the catalyst surface. For Mg–Al HTIs, the structural reconstruction is more complete, and free MgO is present in smaller amounts. Consequently, no significant difference in activity of the parent and reconstructed Mg–Al HTIs is observed.

The stereoselectivity of the alkene is mainly *Z* in all cases, according to the <sup>1</sup>H NMR data. Similar phenomenon was observed for the homogeneous phase under salt-free conditions and using weakly polar solvents such as 1,4-dioxane (Climent et al., 1989). In this case, the catalyst composition only slightly influences the *Z/E* product ratio, which is in the range of 4.0–5.66. The composition and *pK<sub>a</sub>* of the ylide precursor influence the reaction rate and the *Z/E* ratio, as seen in Table 2. When an acidic salt such as Ph<sub>3</sub>P<sup>+</sup>CH<sub>2</sub>COPh (*pK<sub>a</sub>* = 6.0) is used, the reaction was not sensitive to the microcrystalline structure of the catalyst because similar selectivities are obtained in all the cases. This fact can only be explained by assuming that formation of the ylide by the reaction of **2b** with the solid surface is not the rate-controlling step. The very weak acid **3b** gives an unstable ylide (Climent et al., 1989), leading to a much lower reaction rate. These findings are in a good agreement with those reported in the literature (Moison et al., 1987; Climent et al., 1989).

Table 2

Parameters of the Wittig reaction over the Mg5Al sample calcined at 773 K

Aldehyde	Phosphonium salt	<i>pK<sub>a</sub></i> of <b>1b–3b</b>	Reaction time (h)	Yield of <b>1c–3c</b> or <b>4c–6c</b>	<i>Z/E</i> molar ratio
Ph ( <b>1a</b> )	Ph <sub>3</sub> P <sup>+</sup> CH <sub>2</sub> CO <sub>2</sub> Et ( <b>1b</b> )	8.8	1.5	100	90/10
<b>1a</b>	Ph <sub>3</sub> P <sup>+</sup> CH <sub>2</sub> CO <sub>2</sub> Ph ( <b>2b</b> )	6.0	0.5	100	65/35
<b>1a</b>	Ph <sub>3</sub> P <sup>+</sup> CH <sub>2</sub> CH <sub>2</sub> CH <sub>2</sub> CH <sub>3</sub> ( <b>3b</b> )	10–11	6.0	25	85/15
AlCHO ( <b>2a</b> )	<b>1b</b>	8.8	2.0	100	80/20
<b>2a</b>	<b>2b</b>	6.0	0.75	100	60/40
<b>2a</b>	<b>3b</b>	10–11	6.0	15	75/25

Dioxane + water is used as the solvent.

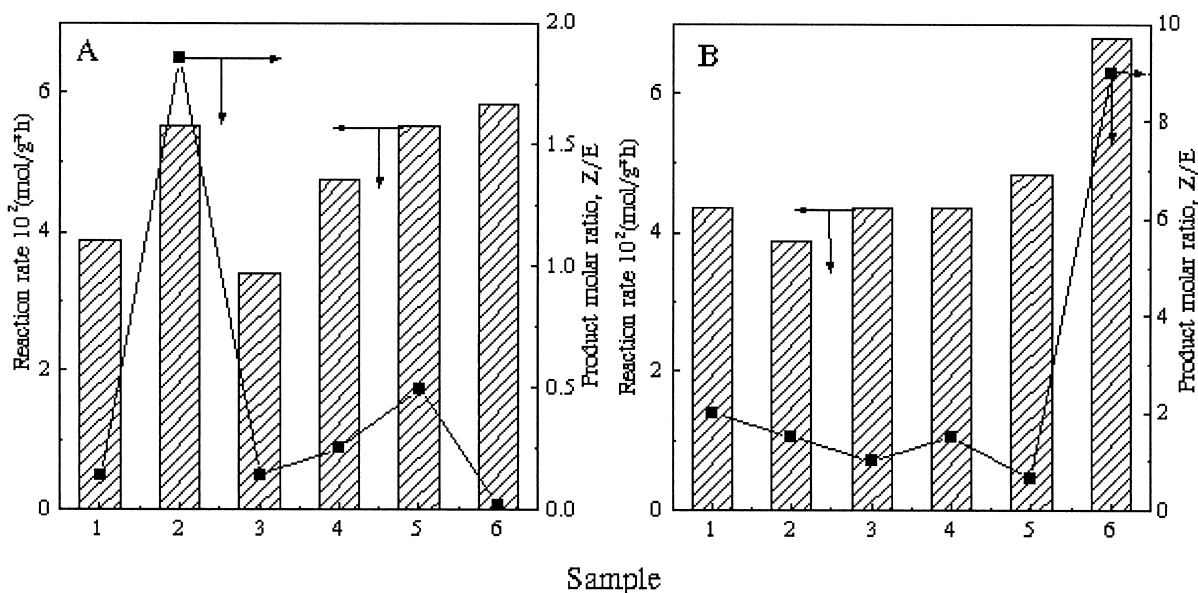


Fig. 5. Influence of the catalyst composition and structural features on activity and selectivity in the Wittig reaction when isobutanol is used as the solvent. A: (1) Mg3Al, (2) Mg3Al (773 K), (3) Mg3Al(R), (4) Mg5Al, (5) Mg5Al (773 K), and (6) Mg5Al(R); B: (1) Zn3Al, (2) Zn3Al (773 K), (3) Zn3Al(R), (4) Zn5Al, (5) Zn5Al (773 K), and (6) Zn5Al(R).

When *i*-BuOH is used as a solvent, contrary to the use of EtOH and dioxane, parent and reconstructed samples exhibit a moderate or high activity (Fig. 5). In this case, the textural features of hydrotalcites insignificantly influence their activity. However, the catalyst selectivity is altered compared to EtOH and especially to 1,4 dioxane. The yield of the *E* alkene noticeably increases (Fig. 5). The behavior of the reconstructed samples is interestingly different. The Mg5Al(R) sample yields mainly *E* (99%) while Zn5Al(R) exhibits the opposite selectivity. We assume that the reaction follows the mechanism proposed by Le Bigot et al. (1986) for the  $K_2CO_3$  catalyzed reaction in a protic solvent. It seems that the polarity of *i*-BuOH controls formation of another transition state (Shen, 1998), leading to a different alkene stereochemistry. It can be explained partially by differences in the hydration behavior between Mg–Al and Zn–Al hydrotalcites, reflecting differences in their surface polarity. Therefore, the use of HTIs in the solid–liquid protic organic medium enabled the synthesis of alkenes of a preferential stereochemistry, i.e. with a high yield of *E*. The aliphatic aldehyde, like heptanal (**2a**), can also be converted over HTIs using the Wittig reaction. The trends of

the catalyst activity and selectivity are similar to those in the case of benzaldehyde.

#### 4. Conclusions

The extent of a structural reconstruction of the calcined HTIs due to a memory effect depends strongly on the heating temperature as well as on their chemical composition. The reconstruction process is complex, and results in the formation of materials with structural and surface features different from those of the parent hydrotalcites.

Hydrotalcites can efficiently catalyze the liquid-phase synthesis of alkenes following the Wittig reaction. The optimum activity was found for materials with the Al/(Al + M<sup>2+</sup>) molar ratio of 0.20–0.26. Their selectivity can be controlled by a proper choice of the pretreatment conditions, such as calcination and structural reconstruction. The solvent composition influences both the reaction rate and catalyst selectivity, and *Z* and *E* alkenes can be obtained with a high yield. The applicability of hydrotalcites for the Wittig reaction is limited by the  $pK_a$  and composition of the ylide precursor. The Wittig reac-

tion is sensitive to the structure of the basic catalyst when a moderate acid, such as  $\text{Ph}_3\text{P}^+\text{CH}_2\text{CO}_2\text{Et}$  with  $pK_a = 8.8$ , is used as the ylide precursor.

## Acknowledgements

The investigations were supported in part by the Ukrainian Ministry of Education, the Polish Committee for Scientific Research (KBN), grant no. 3 TO9A 04714, and by the Schuit Institute of Catalysis, Eindhoven, The Netherlands.

## References

- Beres, A., Palinko, I., Kiricsi, I., Nagy, J., Kiyozumi, Y., Mizukami, F., 1999. Layered double hydroxides and their derivatives—materials for solid base catalysis; synthesis and characterization. *Appl. Catal., A: Gen.* 182, 237–247.
- Cavani, F., Trifiro, F., Vaccari, A., 1991. Hydrotalcite-type anionic clays: preparation, properties and application. *Catal. Today* 11, 173–301.
- Choudary, B.M., Bhumra, V., Narender, N., 1997. Hydrotalcite-like compounds for liquid-phase oxidation of benzylic hydrocarbons. *Indian J. Chem.* 36B, 278–280.
- Climent, M.S., Marinas, J.M., Mouloungui, Z., Le Bigot, Y., Delmas, M., Gaset, A., Sinisterra, J.V., 1989.  $\text{Ba}(\text{OH})_2$  as catalyst in organic reactions: 20. Structure-catalytic activity relationship in the Wittig Reaction. *J. Org. Chem.* 54, 3695–3701.
- Climent, M.J., Corma, A., Iborra, S., Primo, J., 1995. Base catalysis for fine chemicals production: Claisen–Schmidt condensation on zeolites and hydrotalcites for the production of chalcones and flavones of pharmaceutical interest. *J. Catal.* 151, 60–66.
- Climent, M.J., Corma, A., Guil-Lopez, R., Iborra, S., Primo, J., 1999. Solid catalysts for the production of fine chemicals: the use of AIPON and hydrotalcite base catalysts for the synthesis of arylosulfones. *Catal. Lett.* 59, 33–38.
- Hudson, M.J., Carlino, S., Apperley, D.C., 1995. Thermal conversion of a layered (Mg/Al) double hydroxide to the oxide. *J. Mater. Chem.* 5 (2), 323–329.
- Hwang, J.J., Lin, R.-L., Shieh, R.-L., Jwo, J.-J., 1999. Study of the Wittig reaction of benzytriphenylphosphonium salt and benzaldehyde via ylide-mediated phase-transfer catalysis. Substituent and solvent effect. *J. Mol. Catal. A: Chem.* 142, 125–139.
- Kaneda, K., Ueno, S., Imanaka, T., 1995. Catalysis of transition metal-functionalized hydrotalcites for the Baeyer–Villiger oxidation of ketones in the presence of molecular oxygen and benzaldehyde. *J. Mol. Catal. A: Chem.* 102, 135–138.
- Kumbhar, P.S., Sanchez-Valente, J., Lopez, J., Figueras, F., 1998. Meerwein–Ponndorf–Verley reduction of carbonyl compounds catalysed by Mg–Al hydrotalcite. *Chem. Commun.* 535–536.
- Le Bigot, Y., El Gharbi, R., Delmas, M., Gaset, A., 1986. Reactions en milieu heterogene solide–liquide faiblement hydrate III-La reaction de Wittig dans le systeme carbonates alcalins/solvant organique protique. *Tetrahedron* 42 (14), 3813–3823.
- MacKenzie, K.J.D., Meinhold, R.H., Sherriff, B.L., Xu, Z., 1993.  $^{27}\text{Al}$  and  $^{29}\text{Mg}$  Solid-state magic-angle spinning nuclear resonance study of hydrotalcite and its thermal decomposition sequence. *J. Mater. Chem.* 3 (12), 1263–1269.
- Moison, H., Texier-Boullet, F., Foucaud, A., 1987. Knoevenagel, Wittig and Wittig–Horner reactions in the presence of magnesium oxide or zinc oxide. *Tetrahedron* 43 (3), 537–542.
- Rao, K.K., Gravelle, M., Sanchez Valente, J., Figueras, F., 1998. Activation of Mg–Al hydrotalcite catalysts for aldol condensation reactions. *J. Catal.* 173, 115–121.
- Rey, F., Fornes, V., Rojo, J.M., 1992. Thermal decomposition of hydrotalcites. An infrared and nuclear magnetic resonance spectroscopic study. *J. Chem. Soc., Trans.* 88 (15), 2233–2238.
- Shen, Y., 1998. New synthetic methodologies for carbon–carbon double bond formation. *Acc. Chem. Res.* 31, 584–592.
- Soled, S., Levin, D., Miseo, S., Ying, J., 1998. Soft chemical synthesis of mixed molybdate oxidation catalysts and their structural relationship to hydrotalcite. In: Delmon, B., Jacobs, P.A., Maggi, R., Martens, J.A., Grange, P., Poncelet, G. (Eds.), *Preparation of Catalysts VII*. Stud. Surf. Sci. Catal., vol. 118. Elsevier, Amsterdam, pp. 359–367.
- Velu, S., Swamy, C.S., 1994. Alkylation of phenol with methanol over magnesium–aluminium calcined hydrotalcites. *Appl. Catal., A: Gen.* 119, 241–252.
- Watanabe, Y., Tatsumi, T., 1998. Hydrotalcite-like materials as catalysts for the synthesis of dimethyl carbonate from ethylene carbonate and methanol. *Microporous Mesoporous Mater.* 22, 399–407.